Validating the Swiss automatic mesocyclone detection algorithm over the Highveld of South Africa: A case study event

Christina Liesker [1*]; Liesl Dyson[1] and Monika Feldmann[2]
[1]Department of Geography, Geoinformatics and Meteorology, University of Pretoria, Pretoria, South Africa
[2]Institute of Geography, Oeschger Centre for Climate Change Research, University of Bern, Bern, Switzerland
*email: cgthaele@gmail.com

Introduction

Supercell thunderstorms, characterised by a mesocyclone (rotating updraft), peak between October and early December over the Highveld of South Africa (**Fig. 1**)[1]. On 28 November 2013, at least seven supercells moved over the Gauteng Province, causing extensive hail damage. Accurate identification of such events is critical for severe weather warnings. While supercells can be manually identified using Doppler radar, the approach used to create the Radar-Derived Supercell Database (RaD-SD) [1,2] over the Highveld, automatic mesocyclone detection remains novel to South Africa. This study **aims** to evaluate the performance of the Mesocyclone Detection and Tracking (M-DaTing)[3] algorithm developed for Switzerland, in detecting supercells on the Irene S-band Doppler radar using a severe convective event.

Data and methodology

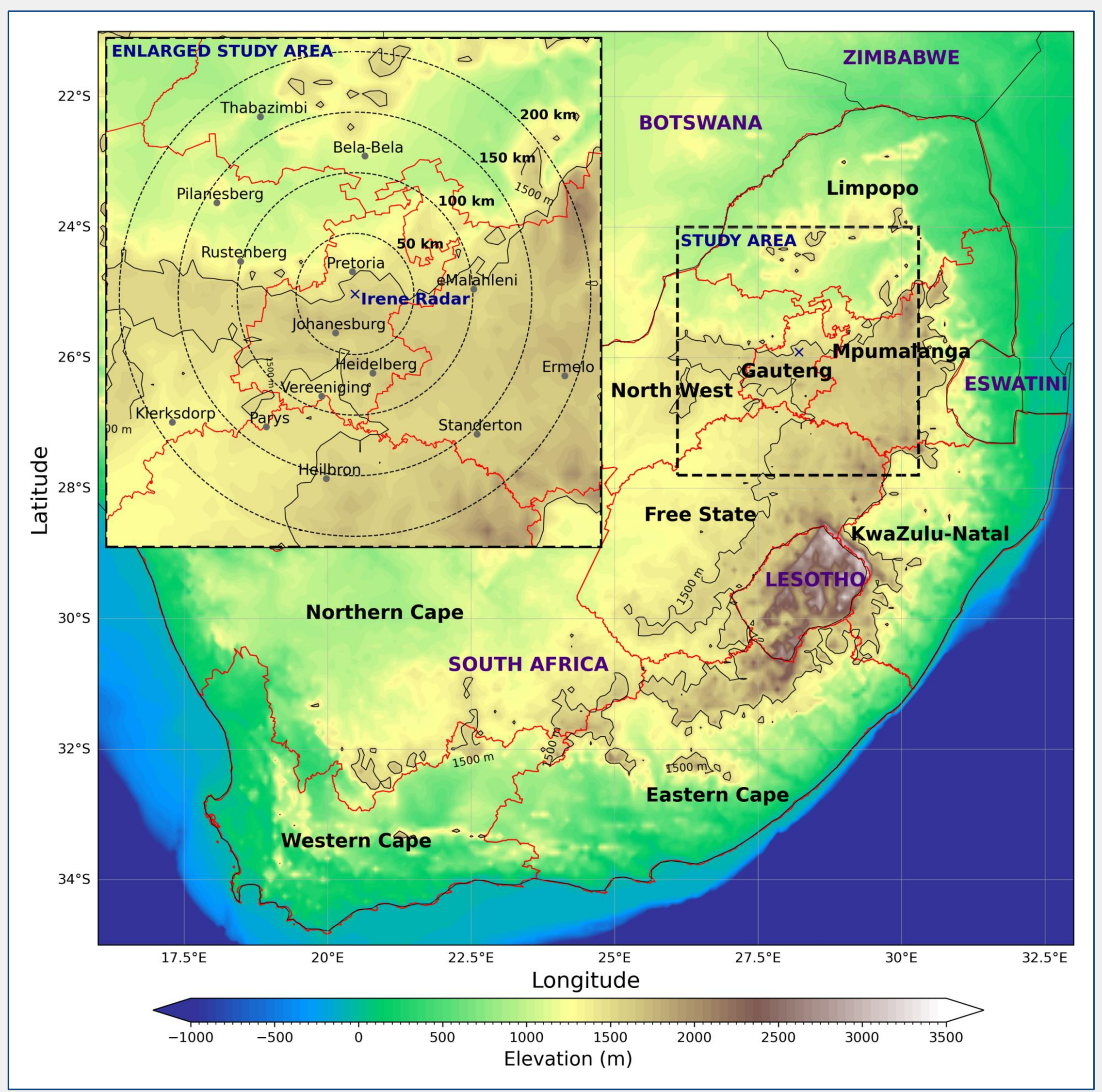

Fig. 1. Topographical and provincial map of South Africa with study area shown. The Highveld is indicated by ≥ 1500 m line.

1. Data and convective event

- Irene S-band single polarised radar (**Fig. 1**).
- 28 November 2013 → complex thunderstorm dynamics.

2. M-DaTing algorithm

- Operational Swiss thresholds.[3]
- Time continuity ± 30 min → to match RaD-SD
- Only negative azimuthal velocity shear (cyclonic rotation) → dominant supercell type in the region.

3. Verification

- M-DaTing results were compared to RaD-SD and reflectivity/velocity fields re-analysed, to ensure no events missed.
- Timesteps/events classified as per **Table 1**.

Table 1. The detection accuracy classification used to evaluate M-DaTing

Classification	Description
TP1	**True Positive.** M-DaTing detected updraft rotation coinciding with a RaD-SD supercell.
TP2	**True Positive.** M-DaTing detected updraft rotation coinciding with a supercell but not within RaD-SD, confirmed through re-analysis.
FP1	**False Positive.** M-DaTing detected rotation not associated with a supercell or not true rotation.
FP2	**False Positive.** M-DaTing detected rotation associated with the poleward flank of a bow echo thunderstorm.
FP3	**False Positive.** M-DaTing detected rotation coinciding with a supercell, but it was spatially misassociated with the updraft.
FN1	**False Negative.** Supercell detected within RaD-SD but not by M-DaTing.
FN2	**False Negative.** Supercell identified through re-analysis but not by M-DaTing.

Results

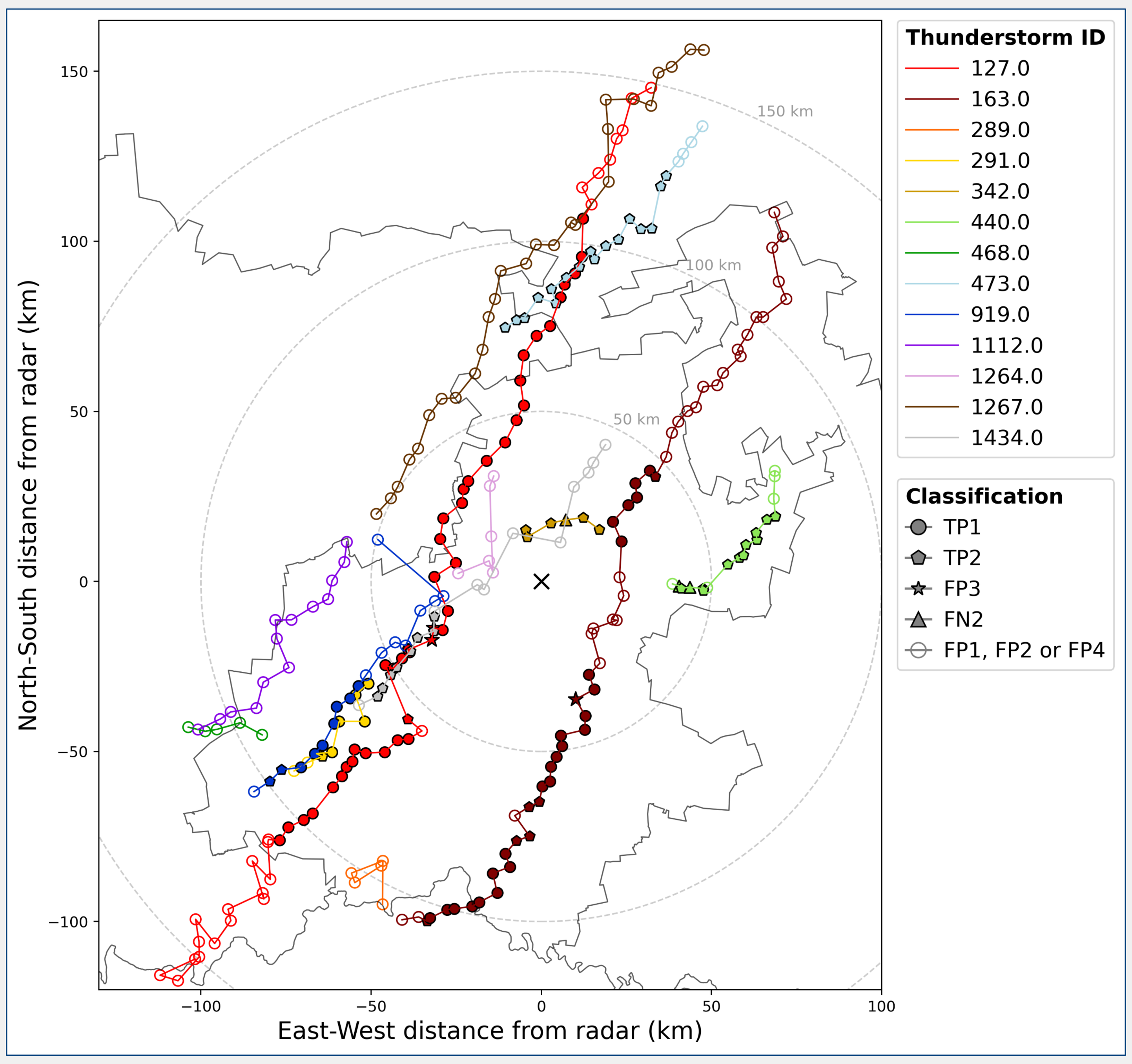

Fig 2. The evaluated M-Dating results on 28 November 2013. Symbols represent classification type (**Table 1**) and average mesocyclone centroid location for each timestep. Colours indicate the thunderstorm IDs and shaded symbols mark supercell events.

1. Highlights

- All seven supercells in RaD-SD were identified by M-DaTing (TP1; **Fig. 2**), and four additional events were detected (TP2; **Fig. 2**).
- Since some events were merged into a single thunderstorm ID, M-DaTing detected a total of eight supercells and five false positive (FP) events.
- There were no full false negatives (FNs), only three FN2 timesteps (**Fig. 2-3**).
- Although there were numerous FP timesteps (FP1-4; **Fig 3**), about 30% corresponded to bow echo rotation (FP2).

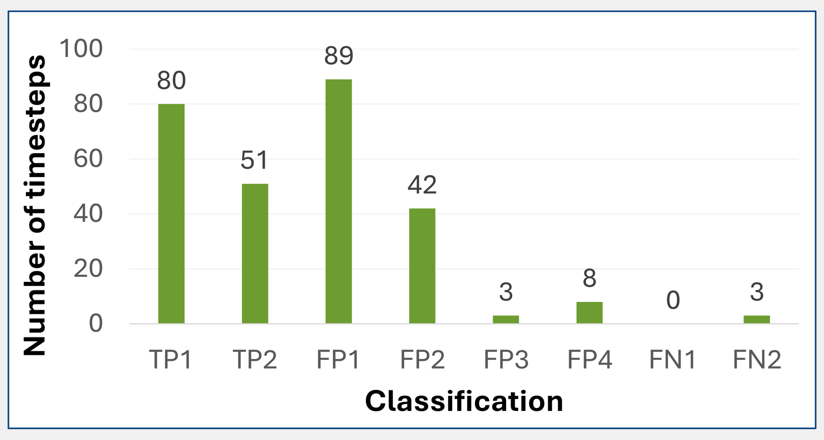

Fig 3. Number of timesteps for each detection accuracy classification (**Table 1**).

2. Detection challenges

- Residual dual-PRF noise.
- Three body scatter spike and beam reflection discontinuities.
- Artificial cropping of velocities due to thunderstorm masks and T-DaTing[3] split/merger issues.
- Vertical continuity discrepancies (**Fig. 4**).
- Clear rotation not detected (**Fig. 5**).

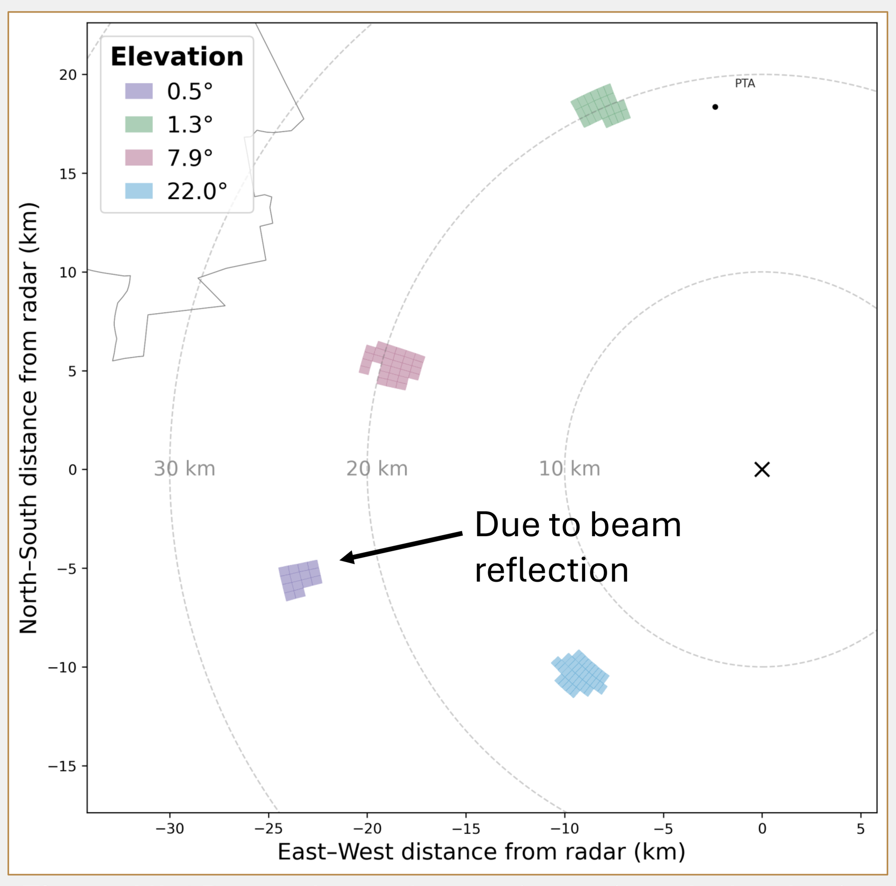

Fig 4. All 2D patches of negative azimuthal velocity shear identified on provided elevations at 18:40 UTC for ID 1264. The 2D patches are not vertically associated and large gaps exist between elevations.

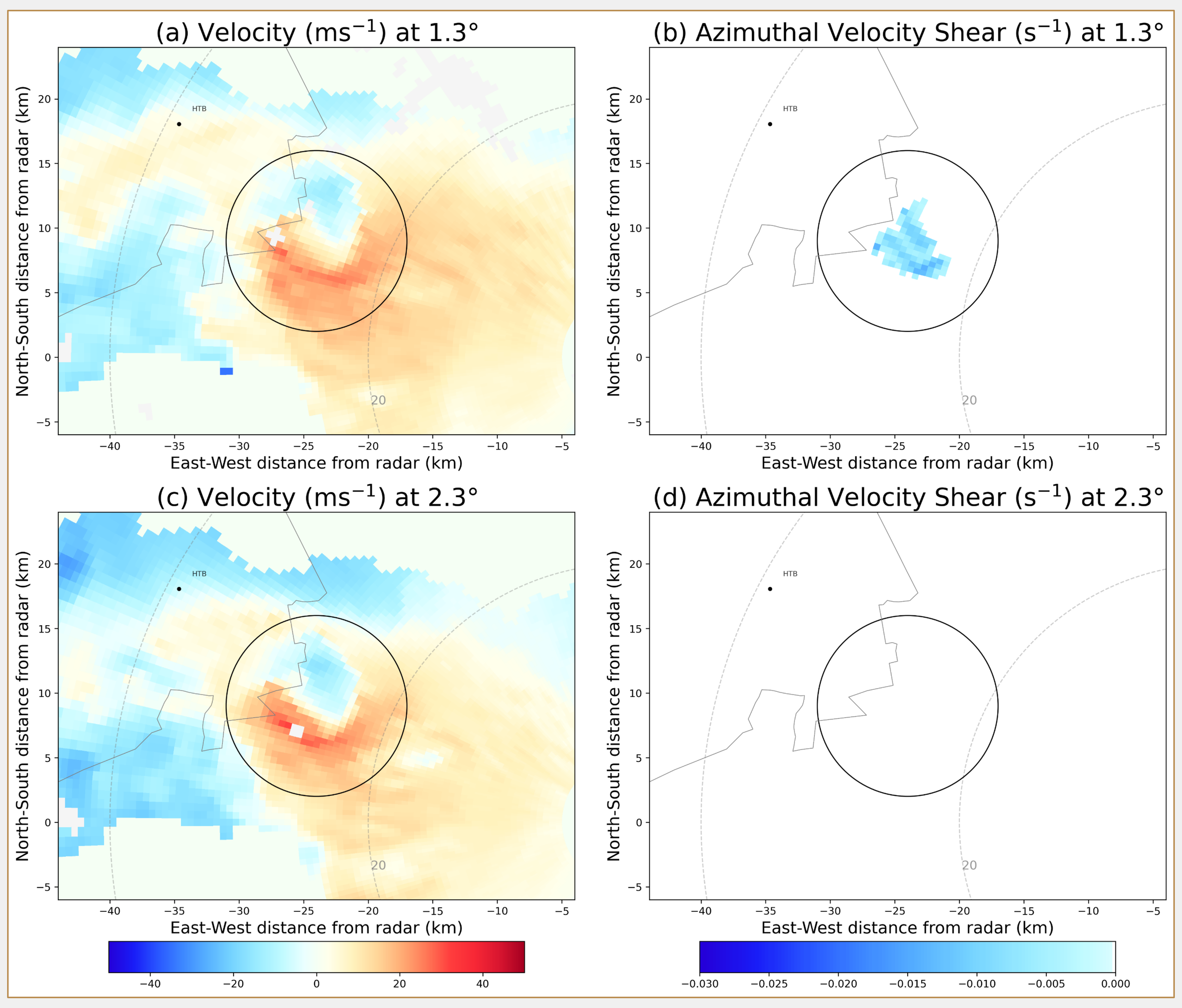

Fig 5. (a), (c) Velocity and (b), (d) 2D patch of negative azimuthal velocity shear at 1.3° and 2.3° for ID 127 at 14:46 UTC. Rotation indicated by the circle. M-DaTing identified rotation at 1.3° but not at 2.3° due to the length to width ratio not meeting the criteria of 1:3.

3. Recommendations

- Noise removal to improve data quality.
- Stricter criteria for vertical stacking.
- Length-to-width ratio was the main reason for FNs, FP3s and missed rotation, thus adjustments required.

Conclusion

M-DaTing **successfully identified all supercell** events during a complex, severe convective case study. However, the false positive rate was relatively high, which may be reduced through improvements to the data quality as well as the algorithm implementation and thresholds. This is a first step towards implementing and testing automatic mesocyclone detection in South Africa. **Future work** will evaluate the algorithm using **all event days** within Rad-SD and making enhancements **to improve** performance and thus readiness for use in severe weather nowcasting and research.

Acknowledgements

- The **South African Weather Service** for use of the Irene S-band Doppler radar data.
- The **Oppenheimer Memorial Trust** for funding this research, which forms part of the main author's PhD.
- The **National Research Foundation** for funding the ECSS2025 conference participation.

References

1. Liesker, C. G., Dyson, L. L. & Becker, E. H., 2024. Characteristics of warm season left-moving supercells over the Highveld of South Africa. Atmos. Res. 300, 107234.
2. [dataset] Liesker, C. G., 2023. Radar-derived supercell thunderstorm database over the Gauteng and Mpumalanga provinces of South Africa from the warm seasons of 2010/2011 until 2019/2020. University of Pretoria.
3. Feldmann, M., Germann, U., Gabella, M. & Berne, A., 2021. A characterisation of Alpine mesocyclone occurrence. Weather Clim. Dyn. 2(4), 1225-1244.

1. 2. 3.